Neutron diffraction studies of structural and magnetic properties of niobium doped cobaltites

2009 J. Phys.: Condens. Matter 21 436002

(http://iopscience.iop.org/0953-8984/21/43/436002)

J. Phys.: Condens. Matter **21** (2009) 436002 (7pp) doi:10.1088/0953-8984/21/43/436002

Neutron diffraction studies of structural and magnetic properties of niobium doped cobaltites

V Sikolenko[1], V Efimov[2], E Efimova[2], A Sazonov[3,4], C Ritter[5], A Kuzmin[6] and I Troyanchuk[7]

[1] Laboratory of Neutron Scattering, ETH Zürich and Paul Scherrer Institute, Villigen, CH-5232, Switzerland
[2] Joint Institute for Nuclear Research, Dubna, RU-141980, Russia
[3] Institute of Crystallography, RWTH Aachen University, Aachen, D-52056, Germany
[4] Research Reactor FRM II, TU Munich, Garching, D-85747, Germany
[5] Institute Laue Langevin, Grenoble, F-39042, France
[6] Institute of Solid State Physics, University of Latvia, Riga, LV-1063, Latvia
[7] Scientific-Practical Materials Research Centre NAS of Belarus, Minsk, BY-220072, Belarus

E-mail: vadim.sikolenko@psi.ch

Received 21 April 2009, in final form 11 September 2009
Published 5 October 2009
Online at stacks.iop.org/JPhysCM/21/436002

Abstract

Neutron powder diffraction studies of the structural and magnetic properties of the $La_{1-x}Sr_xNb_yCo_{1-y}O_3$ solid solutions ($x = 0.2, 0.5$; $y = 0, 0.075, 0.1$) have been performed. Substitution of Co^{2+} by Nb^{5+} prevents the formation of Co^{4+} and leads to stabilization of the Co^{3+} ions in the high- or intermediate-spin state. This is accompanied by the significant change of the Co–O bond length as well as Co–O–Co bond angle in the CoO_6 octahedron. The obtained data are in agreement with the negative sign of the magnetic exchange interactions Co^{3+}–O–Co^{3+} in a relatively wide range of the Co–O–Co bond angles. Diamagnetic dilution by the niobium ions prevents long-range magnetic ordering and strongly increases magnetoresistance at low temperature.

(Some figures in this article are in colour only in the electronic version)

1. Introduction

$La_{1-x}Sr_xCoO_3$ solid solutions attract much interest due to the unusual correlation of their structural, magnetic and transport properties, and also to the spin state transition of the cobalt ions [1]. In the ground state, the parent compound $LaCoO_3$ contains Co^{3+} ions with the low-spin electronic configuration $t_{2g}^6e_g^0$ (LS, $S = 0$). The spin state of Co^{3+} gradually changes to the intermediate (IS, $t_{2g}^5e_g^1$, $S = 1$) or high (HS, $t_{2g}^4e_g^2$, $S = 2$) spin state with an increase of temperature. The redistribution of the electrons between the t_{2g} and e_g levels results from a competition between the crystal field splitting energy Δ_{cf} and the intra-atomic Hund exchange energy J_{ex} which are comparable in cobaltites. The energy Δ_{cf} strongly depends on the Co–O bond length and therefore the balance between Δ_{cf} and J_{ex} can easily be changed by the temperature and external pressure or by a substitution of La for Sr [2–7].

The substitution of trivalent La^{3+} for divalent Sr^{2+} leads to a formation of tetravalent Co^{4+}. Moreover, the ionic radius of Sr^{2+} is much greater than that of the La^{3+} ion and therefore the IS/HS state of Co^{3+} stabilizes [8–11]. These effects modify both the crystal and magnetic structures of the parent compound $LaCoO_3$ and the positive indirect exchange interactions Co^{3+}–O–Co^{4+} establish a long-range ferromagnetic order for $x \geqslant 0.18$ that coincides with insulator-to-metal transition [1–5]. The magnetic phase diagram of $La_{1-x}Sr_xCoO_3$ has been constructed [5]. According to [5] there is a strong tendency to magnetic phase separation.

The origin of the ferromagnetic state in $La_{1-x}Sr_xCoO_3$ has been a subject of debate for a long time. Three main mechanisms for an explanation of the magnetic properties of mixed-valence cobaltites were proposed [8–18]:

- the superexchange model based on the localized electron interaction via an intermediate oxygen ion,

- the Zener double exchange via oxygen and
- the itinerant electron ferromagnetism.

Initially, it was assumed that the double exchange is responsible for the ferromagnetic properties of cobaltites, as in a case of manganites. However, there are many differences in the properties of these two classes of perovskites. For example, the metal–insulator transition and appearance of the long-range ferromagnetic order are well separated from each other in the manganites in contrast to cobaltites where a concentration transition from metal to insulator state occurs simultaneously with the ferromagnetic onset. Moreover, the cobaltites are characterized by 2p-hole conductivity, being negative charge transfer compounds in contrast to manganites.

It is worth noting that the double exchange is not applicable in the case of ferromagnetic compounds where the transition metal ions have the same valence state. However, the mechanism of the exchange interactions between the Co^{3+} ions in the perovskite lattice is not well established. Both dynamic short-range ferromagnetic and more weak antiferromagnetic correlations have been revealed in $LaCoO_3$ at elevated temperature ($T > 100$ K) using elastic and inelastic neutron scattering [19]. In [20], surface ferromagnetism with $T_C \sim 85$ K has been observed in small particles of $LaCoO_3$ with the nominal oxidation state of cobalt ion being 3+. The authors of [17] have proposed three alternative interpretations of the $LaCoO_3$ surface ferromagnetism. In the first model, a part of the Co^{3+} ions are surrounded by five oxygen ions and one OH-group due to the adsorption of water at the crystal surface. The cobalt ions coordinated in this way should reside in the high-spin state without a change of the valence. On the contrary, chemical adsorption of an oxygen atom at a five-fold coordinated site would oxidize the surface cobalt to Co^{4+}. Finally, when trivalent cobalt ions reside in the intermediate-spin state in the CoO_6 octahedra, ferromagnetism can be caused by the e^1–O–e^0 vibronic superexchange between these ions, similar to that in $LaMnO_3$. This model may explain the surface ferromagnetism of $LaCoO_3$. However, bulk ferromagnetism has also been observed recently in epitaxial films [20, 21]. Therefore, further studies are needed to verify the mechanisms of the magnetic interactions between the cobalt ions.

It is possible to increase the Co–O distance and at the same time to keep the 3+ valence state of Co by means of the simultaneous substitution of La^{3+} for Sr^{2+} and Co^{3+} for Nb^{5+}. This changes the spin state of the cobalt ions from LS to IS/HS and therefore leads to enhancement of the magnetic interaction Co^{3+}–O–Co^{3+} [8–11]. The main goal of the present paper is to study the influence of such a complex substitution on the magnetic properties of the parent compound $LaCoO_3$. Therefore, we present here the neutron diffraction, magnetoresistance and magnetization studies of the $La^{3+}_{0.5}Sr^{2+}_{0.5}Nb_yCo_{1-y}O_3$ and $La^{3+}_{0.8}Sr^{2+}_{0.2}Nb_yCo_{1-y}O_3$ series.

2. Experimental details

$La_{1-x}Sr_xCo_{1-y}Nb_yO_3$ ($x = 0.2, 0.5$; $y = 0, 0.075, 0.1$) powder samples were prepared by solid-phase reactions at 1300–1430 °C in air from a mixture of simple oxides and carbonates. Synthesis at higher temperatures favors larger average grain size and better chemical homogeneity of the samples. Phase identification was performed using a powder x-ray diffractometer DRON-3M with Cu Kα radiation at room temperature. X-ray diffraction analysis revealed that all the samples were single phase.

The temperature dependence of magnetization was measured on heating from 2 to 350 K in a magnetic field of 1000 Oe after a field cooling procedure using a commercial Quantum Design's Physical Property Measurement System (PPMS). The magnetotransport properties have been measured using a Cryogen Free Physical Property Measurement System (CRYOGENIC Ltd).

The neutron diffraction experiments for the samples with $x = 0.5$ were performed using three setups: (i) the D1A high-resolution powder diffractometer at the Institute Laue Langevin with the wavelength of incident neutrons $\lambda = 1.91$ Å, (ii) the high-intensity diffractometer D1B with $\lambda = 2.52$ Å, and (iii) the fine resolution diffractometer E9 at the Berlin Neutron Scattering Center (BENSC) of Helmholtz Center Berlin (HZB) [22]. Samples with $x = 0.2$ were studied at the spallation neutron source SINQ at the Paul Scherrer Institute using the high-resolution powder diffractometer HRPT ($\lambda = 1.49$ Å) and the high-intensity diffractometer DMC ($\lambda = 2.45$ Å) [23, 24]. The neutron and x-ray powder diffraction data have been analyzed using the Rietveld method [25] by the FullProf software package [26].

3. Results and discussion

The crystal structure of all the samples can be successfully described in the frame of the rhombohedral space group $R\bar{3}c$. Tables 1 and 2 as well as figure 1 present the unit cell parameters for the studied samples at different temperatures; figure 2 shows an example of the diffraction pattern at 2 K. All structural parameters exhibit a regular thermal expansion; no abnormal structural changes have been found due to temperature change.

Figures 3 and 4 show temperature dependences of the Co–O bond length and Co–O–Co angle for the samples with (a) $x = 0.2$ ($y = 0, 0.1$) and (b) $x = 0.5$ ($y = 0, 0.075, 0.1$). With an increase of niobium content, the unit cell parameters and the Co–O bond length increase, but the Co–O–Co bond angle decreases, i.e. the rhombohedral distortions growth. This can be explained by taking into account the ionic radius of Nb, which is significantly larger than that of Co. Therefore, additional distortions in the Co-sublattice appear with doping. For comparison, we present in figure 3(a) the results from [27] for the pure $LaCoO_3$. At room temperature the Co–O bond length is shorter in $LaCoO_3$ than that in the sample $La_{1-x}Sr_xCo_{1-y}Nb_yO_3$ with $x = 0.2$ and $y = 0.1$, but longer than that in the sample with $x = 0.2$ and $y = 0$. In the $La_{0.8}Sr_{0.2}Co_{0.9}Nb_{0.1}O_3$ sample ($x = 0.2$, $y = 0.1$) the valency of cobalt is 3+ as in $LaCoO_3$, but the Co–O bond is larger and the Co–O–Co angle is smaller.

Elongation of the Co–O bond favors stabilization of the IS or HS state of Co^{3+} ions [8–11]. In other words, the

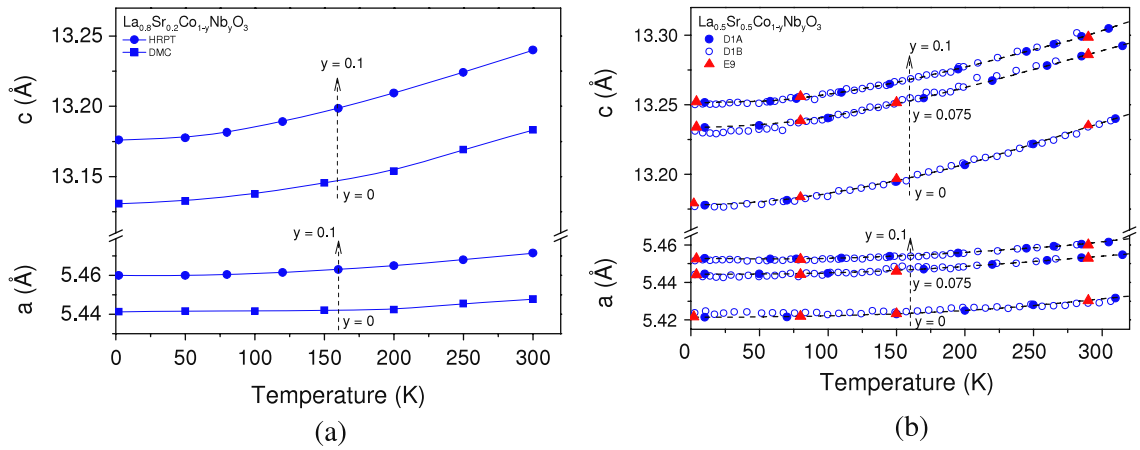

Figure 1. Temperature dependence of the unit cell parameters of (a) $La_{0.8}Sr_{0.2}Co_{1-y}Nb_yO_3$ and (b) $La_{0.5}Sr_{0.5}Co_{1-y}Nb_yO_3$.

Table 1. Structural parameters for $La_{0.5}Sr_{0.5}Co_{1-y}Nb_yO_3$ ($y = 0, 0.075, 0.1$) obtained by the Rietveld refinement of the neutron diffraction data within the space group $R\bar{3}c$ at different temperatures. The cell parameters and the atomic coordinates are given in the hexagonal setting with particular atomic positions La/Sr 6a (0, 0, 1/4), Co/Nb 6b (0, 0, 0), O 18e (0, y, 1/4).

y	0		0.075		0.1	
T (K)	2	290	2	290	2	290
a_h (Å)	5.424 05(5)	5.434 34(8)	5.445 73(5)	5.457 30(5)	5.455 54(5)	5.463 55(5)
c_h (Å)	13.1843(2)	13.2469(3)	13.2373(2)	13.2993(2)	13.2582(2)	13.3071(2)
y [O]	0.4693(2)	0.4745(2)	0.4679(2)	0.4723(2)	0.4667(2)	0.4699(2)
R_B (%)	2.4	3.10	2.95	3.21	2.82	3.12
R_M (%)	8.25	—	8.04	—	15.02	—
μ_{Co} (μ_B)	1.78(3)	—	1.48(4)	—	0.55(9)	—

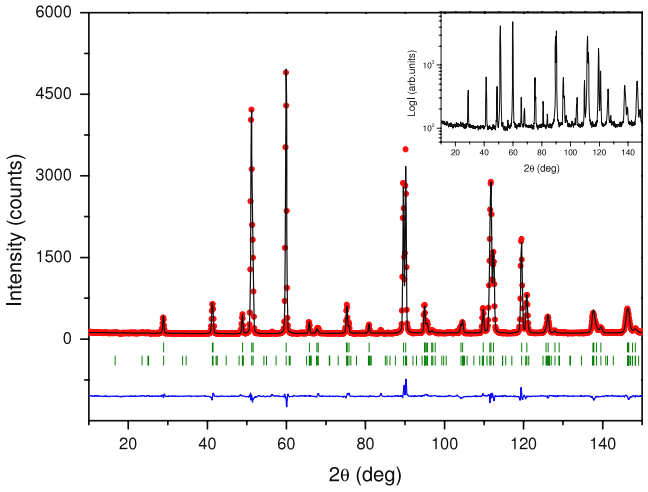

Figure 2. Rietveld refinement of the neutron diffraction pattern for $La_{0.5}Sr_{0.5}CoO_3$ at $T = 2$ K. The circles correspond to experimental data and the solid line represents the calculated pattern. The ticks indicate the calculated nuclear (upper row) and magnetic (lower row) reflection positions. The residual curve is shown at the bottom. Inset shows the pattern in the logarithmic scale.

Table 2. Structural parameters for $La_{0.8}Sr_{0.2}Co_{1-y}Nb_yO_3$ ($y = 0$, 0.1) obtained by the Rietveld refinement of neutron diffraction data within the space group $R\bar{3}c$ at different temperatures. The cell parameters and the atomic coordinates are given in the hexagonal setting with particular atomic positions La/Sr 6a (0, 0, 1/4), Co/Nb 6b (0, 0, 0), O 18e (0, y, 1/4).

y	0		0.1	
T (K)	2	290	2	290
a_h (Å)	5.440 05(3)	5.447 67(3)	5.460 11(4)	5.468 03(4)
c_h (Å)	13.1263(7)	13.1832(6)	13.1759(2)	13.2241(2)
y [O]	0.45645(9)	0.45893(9)	0.45422(7)	0.45640(7)
R_B (%)	1.96	1.76	2.88	2.91
R_M (%)	8.11	—	—	—
μ_{Co} (μ_B)	1.40(3)	—	—	—

cobalt ions in parent $LaCoO_3$ at low temperature adopt a low-spin state while the simultaneously doping by strontium and niobium leads to a stabilization of the higher-spin state due to elongation of the Co–O bond. Doping only by strontium ($y = 0$) results in the opposite effects: as the strontium content increases, the average Co–O bond length decreases while Co–O–Co angle increases, leading to the removal of distortions (figures 3 and 4). This behavior is explained by the increase of the average cobalt oxidation state.

The temperature dependence of the magnetization and of the magnetic moment calculated from the neutron diffraction are in good agreement (see figure 5). For the samples with $x = 0.5$, a decrease of Curie temperature from 240 down to 150 K, as well as a reduction of the magnetic moment of cobalt, have been observed upon increasing niobium content up to $y = 0.1$. For the sample $La_{0.5}Sr_{0.5}Co_{0.9}Nb_{0.1}O_3$, a broad

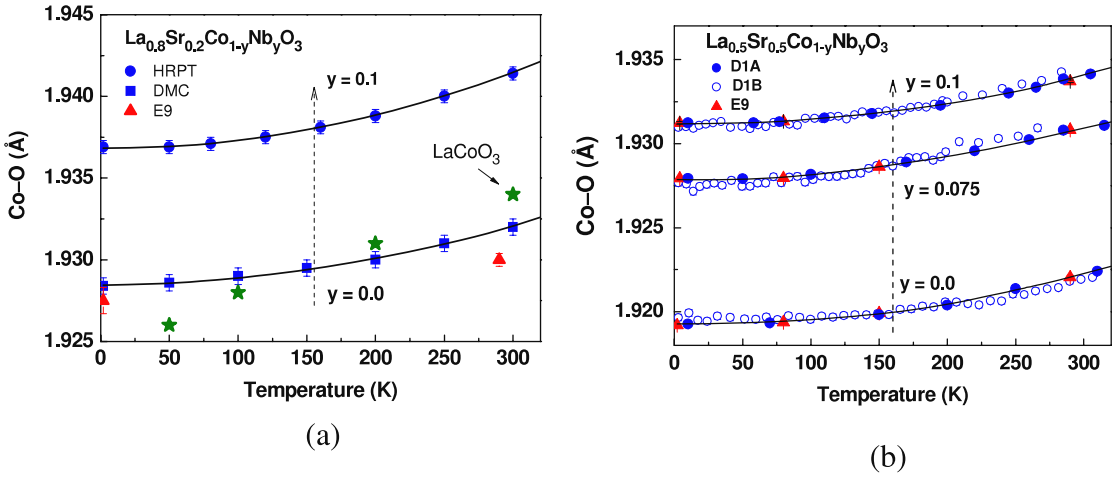

Figure 3. Temperature dependence of the Co–O bond length in (a) $La_{0.8}Sr_{0.2}Co_{1-y}Nb_yO_3$ and (b) $La_{0.5}Sr_{0.5}Co_{1-y}Nb_yO_3$. Data for pure $LaCoO_3$ are taken from [27].

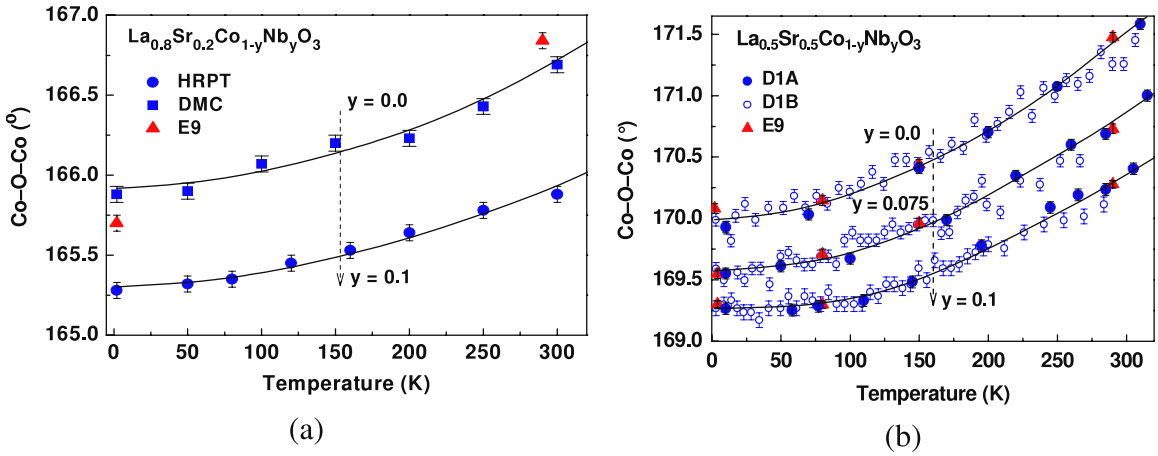

Figure 4. Temperature dependence of the Co–O–Co bond angle in (a) $La_{0.8}Sr_{0.2}Co_{1-y}Nb_yO_3$ and (b) $La_{0.5}Sr_{0.5}Co_{1-y}Nb_yO_3$.

maximum in the temperature dependence of the magnetization in magnetic fields up to 50 kOe was observed around 75–80 K. The magnetization at 80 K is significantly larger than that at 5 K (see figure 6). The coercive force is found to be 80 Oe at 80 K and grows up to 10 kOe at 5 K. This fact implies a sharp increase in the magnetic anisotropy below 80 K. A change of magnetic state is not associated with a structural transition because there is no anomaly in the temperature dependence of the structural parameters (see figures 1, 3 and 4).

The obvious temperature driven change of cobalt spin state has not been revealed by neutron powder diffraction measurements (see figure 5). The calculated magnetic moment is about 0.6 μ_B at 5 K and slightly increases as the temperature rises in the wide temperature range from 5 to 80 K. We suggested that the anomalous behavior of magnetization can be interpreted in terms of the magnetic phase separation scenario proposed for lightly doped insulating cobaltites [5, 28]. This assumption agrees with the temperature dependence of resistivity displayed in figure 7. At temperatures well above the magnetic ordering, the sample demonstrates insulating behavior; ferromagnetic ordering promotes a metallicity, and below 80 K a crossover into the insulating state is observed. The temperature of the reentrant insulating transition almost coincides with the maximum of magnetization (see figure 5). The parent compound $La_{0.5}Sr_{0.5}CoO_3$ exhibits very low magnetoresistance: 2% at 2 K, which increases up to 6% near the Curie point $T_C = 240$ K in a field of 140 kOe [29]. Such behavior of magnetoresistance is typical for heavily doped metallic ferromagnetic cobaltites [30]. A very different magnetoresistance behavior was observed for Nb-doped $La_{0.5}Sr_{0.5}Co_{0.9}Nb_{0.1}O_3$ (see figure 8). In this sample, the magnetoresistance ratio $M(R) = [R(H) - R(H = 0)]/R(H)$ is much larger than that in the parent compound, and it gradually increases upon lowering the temperature without an obvious maximum at the Curie point. This type of magnetoresistance is typical for phase-separated lightly doped insulating cobaltites [28]. It is important to note that the magnetoresistance at 5 K shows magnetic hysteresis in magnetic fields up to 140 kOe, thus indicating a large magnetic anisotropy.

In order to understand the magnetic and magnetotransport properties one can assume that at low temperature the niobium

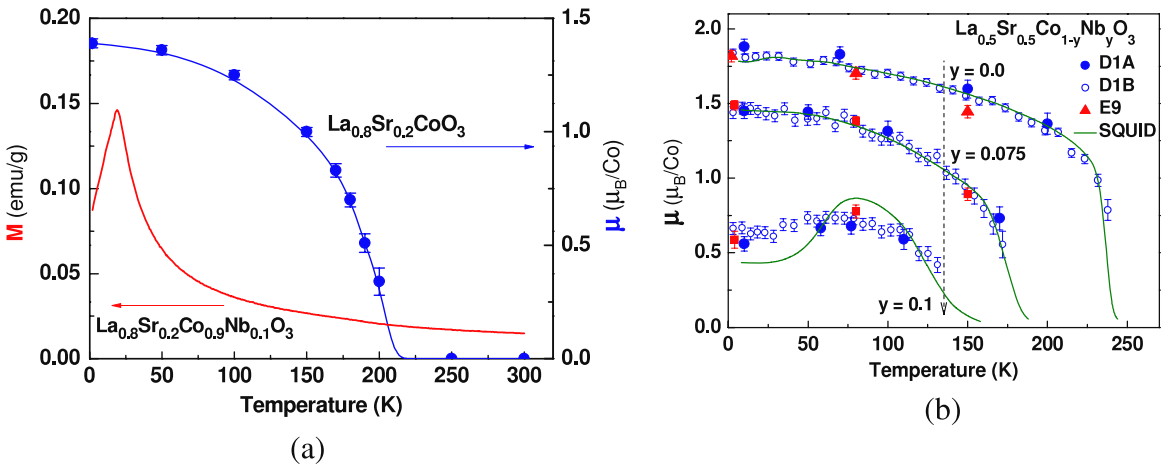

Figure 5. Temperature dependence of (a) magnetization in $La_{0.8}Sr_{0.2}Co_{0.9}Nb_{0.1}O_3$ and magnetic moment in $La_{0.8}Sr_{0.2}CoO_3$, as well as (b) magnetic moment in $La_{0.5}Sr_{0.5}Co_{1-y}Nb_yO_3$ ($y = 0$, 0.075, 0.1)

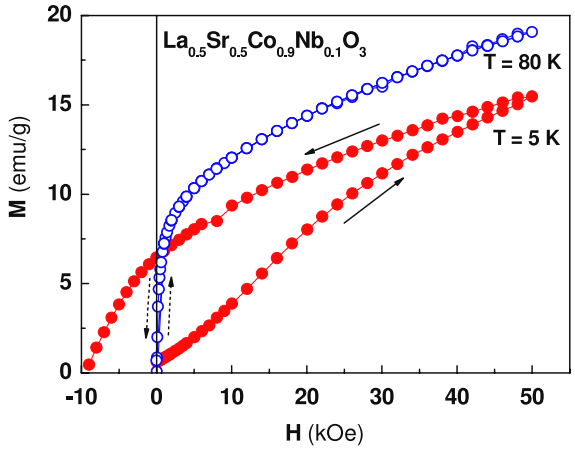

Figure 6. Field dependence of magnetization in $La_{0.5}Sr_{0.5}Co_{0.9}Nb_{0.1}O_3$ at $T = 5$ and 80 K.

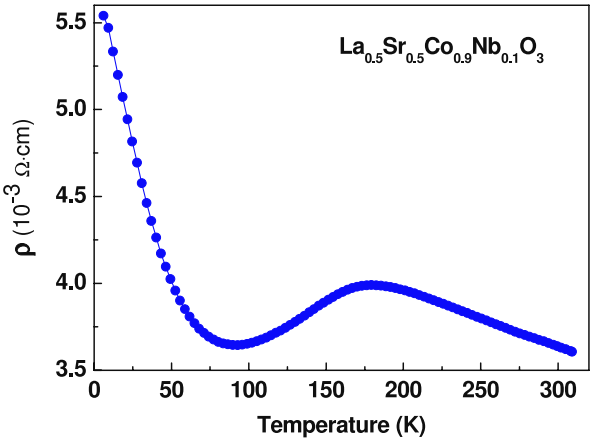

Figure 7. Temperature dependence of resistivity in $La_{0.5}Sr_{0.5}Co_{0.9}Nb_{0.1}O_3$.

doped sample consists of antiferromagnetic clusters embedded in a ferromagnetic matrix, which is not the case for the undoped $La_xSr_{1-x}CoO_3$ parent compound [28]. These clusters arise due to an inhomogeneous distribution of Nb^{5+} ions. Long-range ferromagnetic ordering in the ferromagnetic matrix starts to develop slightly below 150 K (figure 5(b)). In addition, short-range antiferromagnetic ordering in clusters becomes effective at a much lower temperature of about 80 K where a maximum of magnetization and a reentrant transition into the insulating state were observed (figures 6 and 7). Magnetic interactions between antiferromagnetic clusters and the ferromagnetic matrix lead to the frustration of the magnetic bonds at the interface. This leads to a strong increase of magnetic anisotropy and a partial suppression of ferromagnetic order, thus promoting a reentrant insulating behavior. The ferromagnetic matrix can be associated with regions enriched by charge carriers, whereas antiferromagnetic clusters have an insulating character (electronic phase separation). Chemically, the insulating antiferromagnetic clusters should correspond to the domains enriched with Co^{3+} and Nb^{5+}, whereas the conductive ferromagnetic matrix should correspond to the metallic domains with a higher concentration of the Co^{4+} ions. In the antiferromagnetic Co^{3+} enriched clusters, the magnetic interactions between Co^{3+} are dominant, whereas the ferromagnetic state in the matrix results predominantly from ferromagnetic exchange interactions between cobalt in a mixed-valence state, as in the case of $La_{0.5}Sr_{0.5}CoO_3$ having the Curie point of ∼240 K. The giant magnetic anisotropy associated with magnetic hysteresis (figures 6 and 8) implies that the Co^{3+} ions rather adopt the high-spin state than the intermediate one, because in the this case an orbital momentum should be quenched [31]. Note that the unquenched orbital momentum is a source of magnetic anisotropy in magnetically ordered materials.

It is well known that strontium doping of $LaCoO_3$ induces ferromagnetic long-range ordering at $x \sim 0.18$ [2, 3]. The sample $La_{0.8}Sr_{0.2}CoO_3$ has a composition very close to the concentration of the paramagnetic-to-ferromagnetic transition. It shows ferromagnetic ordering with a Curie temperature ∼200 K, whereas in the $La_{0.8}Sr_{0.2}Co_{0.9}Nb_{0.1}O_3$ sample a maximum of zero-field-cooled (ZFC) magnetization is observed near 25 K (see figure 5(a)). Below this temperature, the

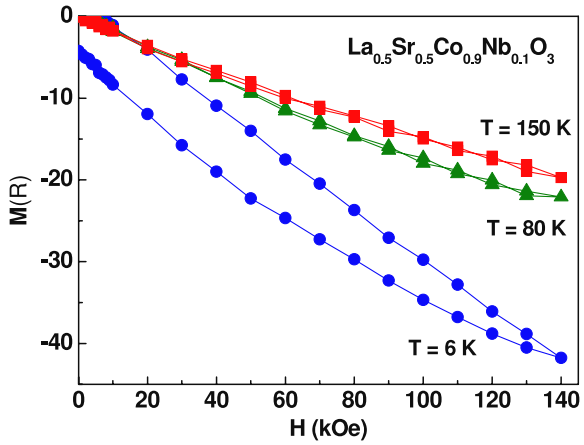

Figure 8. Field dependence of magnetoresistance $M(R) = [R(H) - R(H = 0)]/R(H) \times 100\%$ in $La_{0.5}Sr_{0.5}Co_{0.9}Nb_{0.1}O_3$ at $T = 5$, 80 and 150 K.

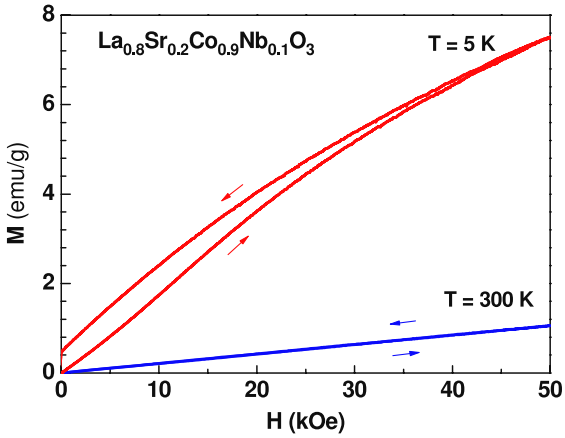

Figure 9. Field dependence of magnetization in $La_{0.8}Sr_{0.2}Co_{0.9}Nb_{0.1}O_3$ at $T = 5$ and 300 K.

field-cooled magnetization becomes much larger than ZFC. No sharp transition into a paramagnetic state has been observed and the FC (ZFC) magnetization curves in relatively low fields are typical for a spin glass. The dependence of magnetization M on magnetic field H in $La_{0.8}Sr_{0.2}Co_{0.9}Nb_{0.1}O_3$ at $T = 5$ and 300 K are shown in figure 9. At 5 K, it does not saturate up to a field of 50 kOe, whereas the absence of remanent magnetization and the linear character of the $M(H)$ curve at 300 K are in accordance with the paramagnetic behavior. Magnetic moments are frozen below 25 K. Above this temperature the remanent magnetization is absent. The spin glass state is in agreement with the neutron diffraction data because a coherent magnetic scattering was not observed. According to the chemical formula, $La_{0.8}Sr_{0.2}Co_{0.9}Nb_{0.1}O_3$ should contain only three-valent cobalt ions. The electrotransport measurements have revealed high resistivity at liquid helium temperature: 10^6 Ω cm, which agrees with a very low concentration of the four-valent cobalt ions in the sample. Simultaneous introduction of Sr^{2+} and Nb^{5+} prevents the appearance of Co^{4+} and favors the Co^{3+} ion transition from the low-spin to a higher-spin state due to an increase of the Co–O bond length [3, 32]. The spin glass state in insulating oxides is a result of competition between antiferromagnetic and ferromagnetic interactions. However, in many cases the spin glass component has been observed in diamagnetically diluted systems with a pure antiferromagnetic or ferromagnetic character of exchange interactions. In the case of $La_{0.8}Sr_{0.2}Co_{0.9}Nb_{0.1}O_3$, the antiferromagnetic interactions are dominant because the paramagnetic Curie point is negative. We believe that the spin glass state for this sample results from an incomplete transition from the low to higher-spin state as well as from diamagnetic dilution by niobium. Our data indicate that in the spin glass $La_{0.8}Sr_{0.2}Co_{0.9}Nb_{0.1}O_3$ and phase-separated $La_{0.5}Sr_{0.5}Co_{0.9}Nb_{0.1}O_3$ the magnetic superexchange interactions Co^{3+}–O–Co^{3+} seem to be predominantly antiferromagnetic.

A ferromagnetic component can be induced in undoped $LaCoO_3$ thin films by epitaxial strain [20, 21]. The ferromagnetism in epitaxial films is not simply a surface property, rather it extends over the whole film thickness, as shown by the linear increase of the saturated magnetic moment with increasing film thickness [20, 21]. The magnetization increases strongly with increasing tensile strain, whereas the transition temperature after a rapid initial rise saturates at $T_C = 85$ K. Since the average Co–O bond length in films practically coincides with that of bulk $LaCoO_3$, the results have been explained by a decrease of the octahedral-site rotation upon increasing tensile strain. The increase of the mean Co–O–Co bonding angle toward 180° leads to an increase of the hybridization of the Co 3d–O 2p orbitals. According to [20, 21] this favors a ferromagnetic superexchange interaction and the population of the higher-spin states. It is important to note that a ferromagnetic component was observed even when a unit cell of the substrate was lower than that of $LaCoO_3$ [21].

In our case, niobium ions, which are much larger than cobalt ions, increase the average Co–O distance in the CoO_6 octahedra, which favors transition of the Co^{3+} ions from the low-spin to higher-spin states. However, doping with Nb ions slightly reduces the Co–O–Co bond angle in contrast to tensile strains in the epitaxial films. In order to explain the available experimental data, one can assume that the sign of the Co^{3+}–O–Co^{3+} superexchange interaction depends on the Co–O–Co bond angle. In this model, increasing the Co–O–Co bond angle should lead to the crossover from an antiferromagnetic to a ferromagnetic character of the magnetic interactions, as was suggested in [21]. However, the sign of magnetic Co^{3+}–O–Co^{3+} interactions is negative in both $La_{0.8}Sr_{0.2}Co_{0.9}Nb_{0.1}O_3$ and $La_{0.5}Sr_{0.5}Co_{0.9}Nb_{0.1}O_3$ despite an increase of the average Co–O–Co bond angle in the CoO_6 octahedron from 165° to 170°, respectively (figure 4). In order to overcome this inconsistency, we assume that strains in small particles and thin films stabilize cobalt in the intermediate-spin state due to distortion of the CoO_6 octahedra. This is possible because the three-valent cobalt ions in the intermediate-spin state experience a Jahn–Teller distortion. The nearest cobalt ions in the intermediate-spin state can interact ferromagnetically with each other through the e^1–O–e^0 vibronic superexchange, as was suggested by Goodenough [17]. However, in standard bulk samples, the elongation of the Co–O bonds stabilizes cobalt in the high-spin state in agreement with recent reports [31, 33]. The 180°

magnetic interactions between these ions in the high-spin state should be antiferromagnetic, in accordance with Goodenough–Kanamori rules. Note that the antiferromagnetic character of Co^{3+}–O–Co^{3+} magnetic interactions has been revealed in $LnBaCo_2O_{5.5}$ (Ln = lanthanide) layered perovskites, where the Co^{3+}–O–Co^{3+} bond angle in the CoO_6-type layer is very close to 170° [34, 35].

4. Conclusions

Neutron powder diffraction studies of the crystal and magnetic structure, as well as magnetoresistance and magnetization measurements, have been performed for $La_{1-x}Sr_xCo_{1-y}Nb_yO_3$ solid solutions with $x = 0.2$ and 0.5 as well as $y = 0.0$; 0.075 and 0.1. A substitution of the cobalt ions by Nb^{5+} prevents Co^{4+} formation and stabilizes the Co^{3+} ions in a higher-spin state. This is accompanied by a significant elongation of the Co–O bond and a slight decrease of the Co–O–Co angle between the neighboring CoO_6 octahedra without altering the $R\bar{3}c$ space group. Nb-doping gradually suppresses the long-range ferromagnetic ordering and metallic character of the resistivity; it also results in a large magnetic anisotropy and giant magnetoresistance. The experimental data have been explained within the model of magnetic (electronic) phase separation. It seems that the nearest Co^{3+} ions, which predominantly adopt the high-spin state, interact antiferromagnetically via the Co^{3+}–O–Co^{3+} superexchange mechanism. No long-range magnetic order arises in $La_{0.2}Sr_{0.2}Co_{0.9}Nb_{0.1}O_3$ due to the incomplete transition of cobalt ions from a low- to high-spin state as well as diamagnetic dilution by the niobium ions.

Acknowledgments

We thank Drs V Pomjakushin and J Purans for their support with experiments and helpful discussions. This work has been supported by the Russian Foundation for Basic Research (grant: 08-02-90053-Bel_a), Fund for Fundamental Research of Belarus (grant F08R-081) and by the European Commission under the 6th Framework Program through the Key Action: Strengthening the European Research Area, Research Infrastructures. Contract no: RII3-CT-2003-505925 (NMI3)

References

[1] Loshkareva N, Gan'shina E, Belevtsev B, Sukhorukov Yu, Mostovshchikova E, Vinogradov A and Krasovitsky V 2003 *Phys. Rev.* B **68** 024413
[2] Sikolenko V, Sazonov A, Troyanchuk I, Többens D, Zimmermann U, Pomjakushina E and Szymczak H 2004 *J. Phys.: Condens. Matter* **16** 7313
[3] Sazonov A, Troyanchuk I, Sikolenko V, Chobot G and Szymczak H 2005 *J. Phys.: Condens. Matter* **17** 4181
[4] Fita I, Mogilyansky D, Markovich V, Puzniak R, Wisniewski A, Titelman L, Wradman L, Herskowitz M, Varyukhin V and Gorodetsky G 2008 *J. Non-Cryst. Solids* **354** 5204
[5] Wu J and Leighton C 2003 *Phys. Rev.* B **67** 174408
[6] Efimov V *et al* 2007 *Phys. Status Solidi* c **4** 805
[7] Efimova E *et al* 2008 *J. Phys. Chem. Solids* **69** 2187
[8] Goodenough J 1971 *Mater. Res. Bull.* **6** 967
[9] Senaris-Rodriguez M and Goodenough J 1995 *J. Solid State Chem.* **118** 323
[10] Louca D, Sarrao J, Thompson J, Roder H and Kwei G 1999 *Phys. Rev.* B **60** 10378
[11] Korotin M, Ezhov S, Solovyev I, Anisimov V, Khomskii D and Sawatzky G 1996 *Phys. Rev.* B **54** 5309
[12] Troyanchuk I 1992 *J. Exp. Theor. Phys.* **75** 132
[13] Zenner C 1951 *Phys. Rev.* **81** 440
[14] Jonker G and Van Santen J 1953 *Physica* **19** 120
[15] Goodenough J 1958 *J. Phys. Chem. Solids* **6** 287
[16] Kopcewicz M, Karpinsky D and Troyanchuk I 2005 *J. Phys.: Condens. Matter* **17** 7743
[17] Yan J Q, Zhou J S and Goodenough J B 2004 *Phys. Rev.* B **70** 014402
[18] Raccah P and Goodenough J B 1967 *Phys. Rev.* B **155** 932
[19] Phelan D *et al* 2006 *Phys. Rev. Lett.* **96** 027201
[20] Fuchs D, Pinta C, Schwarz T, Schweiss P, Nagel P, Schneider R, Merz M, Roth G and Lohneysen H 2007 *Phys. Rev.* B **75** 144402
[21] Fuchs D, Arac E, Pinta C, Schuppler S, Schneider R and Lohneysen H 2008 *Phys. Rev.* B **77** 014434
[22] Többens D, Stüßer N, Knorr K and Lampert G 2001 *Mater. Sci. Forum* **288** 378
[23] Fisher P, Frey G, Koch M, Könnecke M, Pomyakushin V, Schefer J, Thut R, Schlunpf N and Greuter U 2000 *Physica* B **276–278** 146
[24] Fisher P, Keller L, Schefer J and Kohlbrecher J 2000 *Neutron News* **11** 19
[25] Rietveld H 1969 *J. Appl. Crystallogr.* **2** 65
[26] Rodriguez-Carvajal J 1992 *Physica* B **55** 192
[27] Radaelli P G and Cheong S W 2002 *Phys. Rev.* B **66** 094408
[28] Wu J, Lynn J W, Glinka C J, Burley J, Zheng H, Mitchell J F and Leighton C 2005 *Phys. Rev. Lett.* **94** 037201
[29] Mahendiran R and Raychaudhuri A 1996 *Phys. Rev.* B **54** 16044
[30] Stauffer D D and Leighton C 2004 *Phys. Rev.* B **70** 214414
[31] Haverkort M W *et al* 2006 *Phys. Rev. Lett.* **97** 176405
[32] Stolen S, Gronvold F, Brinks H, Atake T and More H 1997 *Phys. Rev.* B **55** 14103
[33] Podlesnyak A, Streule A, Mesot J, Medarde M, Pomjakushina E, Conder K, Tanaka A, Haverkort M and Khomskii D 2006 *Phys. Rev. Lett.* **97** 247208
[34] Troyanchuk I, Karpinsky D and Yokaichiya F 2008 *J. Phys.: Condens. Matter* **20** 335228
[35] Pomjakushina E, Conder K and Pomjakushin V 2006 *Phys. Rev.* B **73** 113105